ACS NANO
Cite This: ACS Nano 2018, 12, 11229–11235
www.acsnano.org

ARTICLE

Molecular Orbital Gating Surface-Enhanced Raman Scattering

Chenyang Guo,[†,▽] Xing Chen,[‡,▽] Song-Yuan Ding,[§,▽] Dirk Mayer,[∥] Qingling Wang,[†] Zhikai Zhao,[†,⊥] Lifa Ni,[†,#] Haitao Liu,[†] Takhee Lee,[*,⊥] Bingqian Xu,[*,#] and Dong Xiang[*,†]

[†]Tianjin Key Laboratory of Optoelectronic Sensor and Sensing Network Technology, Key Laboratory of Optical Information Science and Technology, Institute of Modern Optics, College of Electronic Information and Optical Engineering, Nankai University, Tianjin 300071, China

[‡]Department of Chemistry, The Pennsylvania State University, State College, Pennsylvania 16802, United States

[§]State Key Laboratory of Physical Chemistry of Solid Surfaces (PCOSS), Collaborative Innovation Centre of Chemistry for Energy Materials (iChEM), and Department of Chemistry, College of Chemistry and Chemical Engineering, Xiamen University, Xiamen 361005, China

[∥]Peter-Grünberg-Institute PGI-8, Bioelectronic Research Center Jülich GmbH and JARA Fundamentals of Future Information Technology, Jülich 52425, Germany

[⊥]Department of Physics and Astronomy, Seoul National University, Seoul 08826, Korea

[#]College of Engineering, University of Georgia, Athens, Georgia 30602, United States

Supporting Information

ABSTRACT: **One of the promising approaches to meet the urgent demand for further device miniaturization is to create functional devices using single molecules. Although various single-molecule electronic devices have been demonstrated recently, single-molecule optical devices which use external stimulations to control the optical response of a single molecule have rarely been reported. Here, we propose and demonstrate a field-effect Raman scattering (FERS) device with a single molecule, an optical counterpart to field-effect transistors (a key component of modern electronics). With our devices, the gap size between electrodes can be precisely adjusted at subangstrom accuracy to form single molecular junctions as well as to reach the maximum performance of Raman scattering via plasmonic enhancement. Based on this maximum performance, we demonstrated that the intensity of Raman scattering can be further enhanced by an additional ∼40% if the orbitals of the molecules bridged two electrodes were shifted by a gating voltage. This finding not only provides a method to increase the sensitivity of Raman scattering beyond the limit of plasmonic enhancement, but also makes it feasible to realize addressable functional FERS devices with a gate electrode array.**

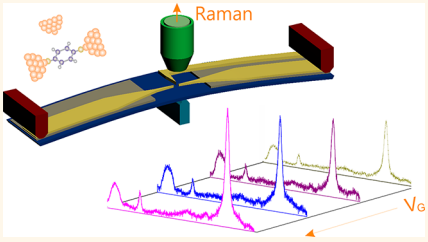

KEYWORDS: *molecular electronics, molecular devices, Raman scattering, nanogaps, limit of plasmonic enhancement*

Molecular electronic devices, in which individual molecules are utilized as active electronic components, are promising for the ultimate miniaturization of electronic devices.[1−5] In particular, building single-molecule field-effect transistors (FETs) is considered as a critical step in realizing real data-processing by means of molecular devices. Single-molecule FETs have been made by several research groups, in which the current in the molecular junctions was modulated by a gate voltage.[6−8] Meanwhile, several *in situ* characterization methods with single-molecule sensitivity have been developed, enabling an in-depth understanding of molecule electronics.[9−12] Among the characterization methods, Raman spectroscopy is particularly regarded as a powerful tool in both chemistry and physics because it can be integrated into electrical measurements to add critical chemical fingerprint information on the molecules into the electronic properties.[13−19] A major task of such research is to achieve maximum sensitivity of the Raman spectroscopy, and several strategies have recently been proposed to increase the sensitivity of Raman scattering.[20−27] However, gating of single-molecule Raman spectroscopy, which promotes the sensitivity of Raman spectroscopy not only as a characterization tool but also as a functional molecular optical device, has not been reported due to the tremendous challenges involved:[10,28] (1) lacking a reliable method to bridge the single molecule between the source and drain electrodes and stabilize

Received: July 31, 2018
Accepted: October 15, 2018
Published: October 15, 2018

DOI: 10.1021/acsnano.8b05826
ACS Nano 2018, 12, 11229–11235

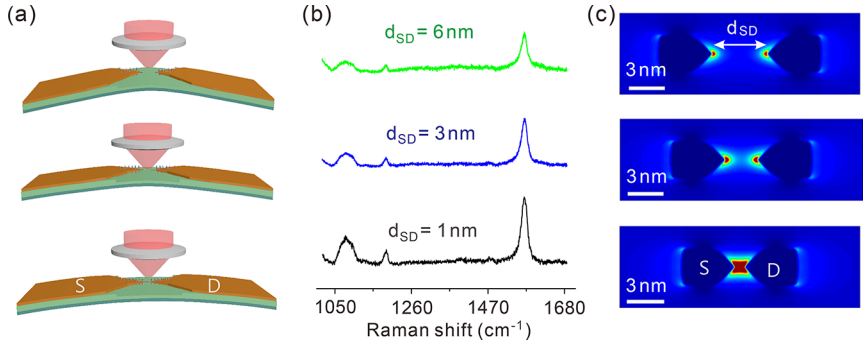

Figure 1. Gap size dependence of Raman spectroscopy with 1,4-benzenedithiol. (a) Schematic drawings of the approximate 6, 3, and 1 nm gap sizes that were achieved by relaxing the substrate. (b) SERS of 1,4-benzenedithiol corresponding to the gap sizes shown in (a). The Raman signal was enhanced as the gap size decreased and reached its pinnacle for $d \sim 1$ nm. (c) Simulations of the electric field distribution due to an incident laser as the gap size varied from 6 to 1 nm. The incident light (λ = 632.8 nm) is polarized along nanodimer axis and creates the maximal field in the center of gap. The field was enhanced and confined with gap shrinking.

for long time; (2) ensuring the signals from the target single molecule are dominant over those of the substantial surrounding molecules (in other words, hot spots should be generated to sensitively probe target single molecules); and (3) integrating a gate electrode, a few nanometers away from the target molecule, into the molecular junction to generate the required gating effect.

Herein, we propose a side-gated Raman scattering approach where the mechanically controllable break junction technique was employed to realize FERS. With this system, we can gradually confine the electromagnetic field to the vicinity of the molecular junction via precise gap modulation, allowing the acquisition of distinct Raman signals from the molecular junction from the background signals from surrounding molecules. More significantly, this Raman scattering of a single molecular junction can be further enhanced by an additional ~40% via the effect of the gate voltage when the field enhancement caused by the gap modulation has reached its maximum. Combining the tunneling current measurements and simulations, we revealed the chemical enhancement mechanism predominately contributes to the side-gated Raman scattering as a result of the gate-voltage tuning of the molecular energy levels.

RESULTS AND DISCUSSION

Gap Control of Electromagnetic Enhanced Raman Scattering. Mechanically controllable break junctions (MCBJs)[29−31] combined with surface-enhanced Raman scattering (SERS)[14,32,33] were used to address the electromagnetic enhancement limitation via gap modulation. The MCBJ (see Figures S1 and S2) allowed us to precisely control the gap size between the electrodes over the range of a few angstroms to several nanometres, with a subangstrom resolution.[34−36] The incident laser was focused onto the molecular junction through a lens from the top of the MCBJ chip, and the scattered light was collected using the same lens and was directed to a spectrometer; see Figure S3. We first examined the Raman intensities at different spots on the electrodes surface by laser scanning along the electrodes axis. We found that the SERS signals from the gap area are much stronger than those from elsewhere, which agrees with the previous reports,[10,23,32] indicating that SERS signals from the molecules trapped in between the two electrode apexes are significantly enhanced. Subsequently, we examined the impact of the incident light polarization on the SERS signal. We found that the SERS intensity increases ~30% when the source-drain electrodes are rotated from the parallel direction to the perpendicular direction with respect to the laser polarization (see Figure S4). The observed polarization dependence provides evidence that molecules inside the nanogap are indeed mainly responsible for the SERS signal because SERS from flat surfaces outside the gap region should be polarization independent.

Figure 1a,b clearly shows that the SERS intensity correlated highly with the gap sizes. Specifically, the SERS intensity increased gradually when the gap size was reduced from 6 to 1 nm. This observation is reasonable since the electromagnetic field increases dramatically as the gap size between two nanoelectrodes is reduced. Figure 1c shows the electric field distribution simulated using the atomistic electrodynamics model. A cutoff value is used to unify the electric distributions for different gaps in the scale bar; see Figure S5. The simulated results clearly show that the electric field was greatly enhanced and confined in the gap regime while the gap size was decreased. The simulation results also show that the "hottest spot" appears in the plasmonic junction when the gap separation is reduced (particularly at ~1 nm). According to the electromagnetic enhancement mechanism, *i.e.*, the enhancement factor is roughly estimated by the magnitude of local field to fourth power, the enhanced Raman spectra from the molecules trapped in the nanogap will overwhelm the Raman signals from elsewhere.

Figure 2a shows the scanning electron microscopy (SEM) image of a representative MCBJ sample whose size of the suspended constriction part is approximate 40 nm × 40 nm. This constriction will be elongated until a finally break, *i.e.*, a gap will appear after the break of constriction upon the bending substrate.[37] Figure 2b shows the Raman intensity at 1568 cm^{-1} (the band at approximately 1568 cm^{-1} was chosen as a representative vibrational mode) as a function of the gap size between the source and drain electrodes. Raman intensity apparently increases as the gap size decreases from 6 to 1 nm. Interestingly, the growth saturates when the gap is further reduced from 1 to 0.1 nm. This observation can be attributed to the ultimate limits of plasmonic enhancement arising from the electron tunneling between the two electrode tips.[22,38−40]

Beyond the Electromagnetic Enhancement via Molecular Orbital Gating. In a single-molecule FET, the electron transport properties can not only be tuned using the bias voltage between the source and drain electrodes but also

DOI: 10.1021/acsnano.8b05826
ACS Nano 2018, 12, 11229−11235

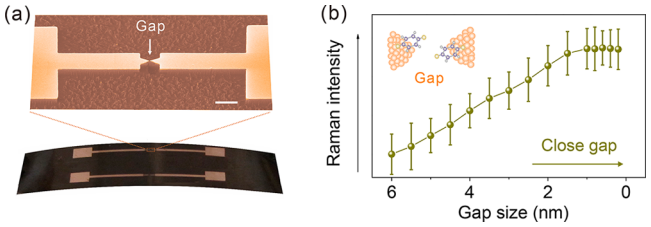

Figure 2. Intensity of the SERS as a function of the gap size. (a) SEM image of a MCBJ chip fabricated on a relaxed spring steel substrate using e-beam lithography and reactive ion etching. A gap was generated when the substrate was bent. This gap size can be precisely controlled at subangstrom accuracy by the bending of the substrate. Scale bar: 1 μm. (b) Raman intensity (@ 1568 cm^{-1}) decreases as gap size increases and gradually approaches the maximum at $d \sim 1$ nm.

be tuned by the gate voltage. In our MCBJ-SERS design, a side-gate electrode perpendicular to the source and drain electrodes was integrated into MCBJ chips to realize the side-gated SERS (see details in Figure S6). Notably, the side gate electrode perpendicular to the source-drain electrodes will not undergo any stretching force during the substrate bending process (Figure 3a). Therefore, the gate electrode remains undamaged upon the bending of substrate, which is unavailable for those junctions with bottom- or top-gate electrode configurations.

To obtain a single-molecule junction, the gap size was precisely decreased and the tunneling current was monitored simultaneously. Approximate 10% of the current/distance traces showed current jump features during the gap shrinking. In contrast, no current jump was observed with bare electrodes (without assembled molecules on the electrodes surface); see Figure 3b. The current jump indicates the onset of the first molecule attaching to the opposite electrode, forming a single molecular junction. Once the current jump occurred, we immediately fix the gap size and withhold the junction while simultaneously performing Raman measurements under different gate voltages. Figure 3c shows the SER spectra of 1,4-benzenedithiol upon various gate voltages when a fixed bias voltage (V_b = 0.1 V) was applied to the source-drain electrodes. Interestingly, the Raman intensity increased as the gate voltage changes from 0 to −20 V, although no shifting of vibrational frequencies was observed. We attribute the gating effects to the molecular orbital shifting by the gate voltage (we will address this point later in more detail). To confirm, we further performed the measurements of the tunneling current under the different gate voltages, by which compelling evidence for the orbital shift was obtained.

Figure 3d shows the $I-V$ curves of a single molecular junction as a function of the gate voltage. For chips whose distance between the gate electrode and source-drain electrodes is less than 10 nm, 12 out of 67 junctions showed the FET behavior. We found that the conductance of the molecular junctions increased as the gate voltage changes to more

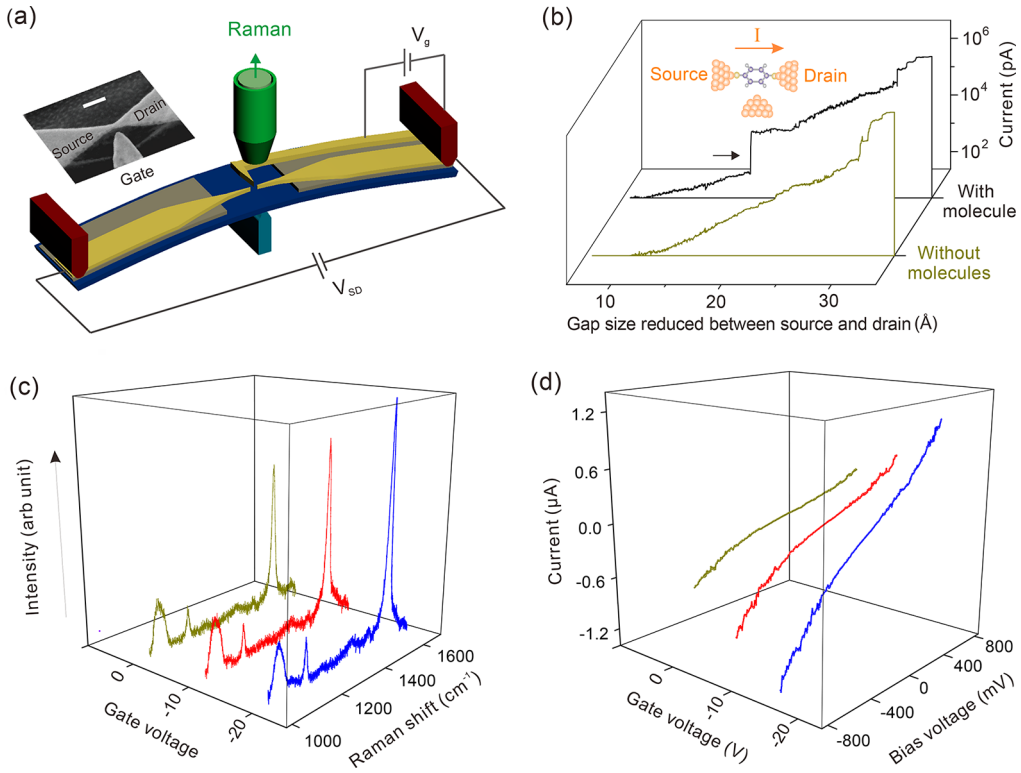

Figure 3. Raman spectra and tunneling current of 1,4-benzenedithiol depend on the gate voltage. (a) Schematic illustration of the measurement system for side-gating Raman scattering. Inset: SEM image of a MCBJ chip with a side-gate electrode, in which the nanoconstriction will break upon the bend of substrate. Scale bar: 100 nm. (b) Current curves recorded during the electrode approach process with and without assembled molecules. V_{bias} = 100 mV. A current jump was observed when the molecules were presented. Inset: Schematic illustration of a single-molecule junction with a side-gate electrode formed during the electrode approach process. (c) SERS spectra recorded when the bias voltage between the source and drain electrodes is fixed at 100 mV and (d) $I-V$ curves of 1,4-benzenedithiol molecular junction upon different gate voltages.

DOI: 10.1021/acsnano.8b05826
ACS Nano 2018, 12, 11229−11235

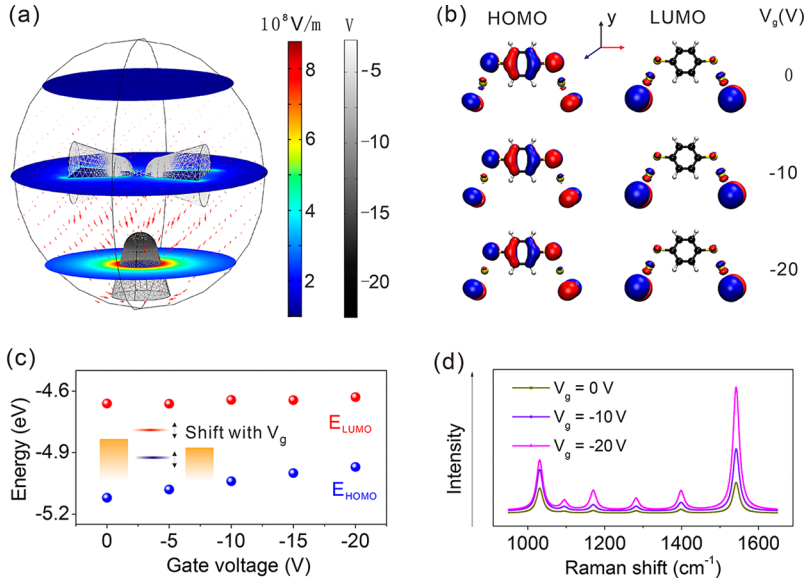

Figure 4. Electric field simulation and SERS calculation upon side-gate voltage. (a) Simulation of the electric field distribution with source-drain voltage of 12 mV and gate voltage of −20 V. Arrows indicate the directions of the electric field vector. Left color bar shows the electric field strength distribution of the three cross sections, and right color bar presents the potential distribution the electrode surface. (b) Gate voltage dependence of the spatial distribution of the molecular orbital for 1,4-benzenedithiol molecular junctions. Orbitals in blue and red indicate the positive and negative wave function amplitudes, respectively. Black arrow indicates the *y*-axis (electric direction). (c) Dependence of HOMO and LUMO energy shift on the applied gate voltage. A negative gate voltage would raise the orbital energies of the molecules relative to the Fermi level of the electrodes (E_F). Inset: energy diagram of the gold−BDT−gold junction. (d) Simulated Raman spectroscopy as a function of the gate voltage.

negative values. This FET behavior provides direct evidence that the energy barrier for the electron tunneling through the metal−molecule−metal junction was reduced upon the gate voltage due to the molecular orbitals shifting. In contrast, without molecules in the gap, we never observed the FET behavior (see Figure S7). The low yield (∼18%) of devices that demonstrated FET behaviors is because the gate efficiency is extremely sensitive to the exact position of molecules with respect to the gate electrode, which is difficult to control. For those molecules that are bridged between the source and drain electrodes while residing at the back side of the source-drain electrodes with respect to the gate electrode, the FET behavior will not be observed due to the field screening effect.[41] Notably, for the molecular junctions in the absence of the electrical FET behavior, there is no gating controls of the Raman intensities.

Additionally, we have not observed the Raman scattering gating effect of the molecular junctions using the molecules with only one end bond group. In other words, we only observed the gating effect when the two electrodes were bridged by molecules with two end bond groups. We attribute this observation to the fact that the energy gap between HOMO and LUMO was reduced due to the hybridization of molecular and metal electronic states when the molecule bridge was formed. Because the Raman enhancement factor is inversely proportional to the fourth power of the excitation energy (positively related to the energy gap between HOMO and LUMO),[42] the Raman signal contribution from those molecules bridged two electrodes will be strongly affected by the gate voltage.

To further clarify and understand how the molecular orbitals are affected by the gate voltage, we performed first-principle calculations based on density functional theory (DFT). First, we calculated the electric field strength and the potential distribution around the nanoelectrodes when the gate voltage was applied. The simulations showed that both the field and the potential distribution were highly inhomogeneous and strongly dependent on the location of the gate electrode with respect to the source and drain electrodes (see Figures 4a and S8). The averaged electric field and the potential in the gap were extracted and used as input for the subsequent DFT calculations of the molecular orbitals and Raman spectra. The geometry optimization was performed using the Becke-Perdew (BP86) functional and the vibrational frequencies and normal modes were calculated under the harmonic approximation. All calculations were carried out using the Amsterdam density functional (ADF) program package; see the Supporting Information for detailed information. Figure 4b shows the frontier molecular orbitals under different gate voltages. We do not find substantial changes in the HOMO and LUMO with the applied gate voltage aligned with the *y*-axis, which means that the gate voltage rarely changes the main electronic configuration of 1,4-benzenedithiol in the range from −20 to 0 V. However, the applied gate voltage significantly modifies the energy gap between the HOMO and the LUMO as shown in Figure 4c. Both the E_{HOMO} and the E_{LUMO} are up-shifted as the gate voltage is negatively increased. With a close examination of Figure 4c, we found that the energy shifts for the HOMO and the LUMO are different at a given gate voltage. The HOMO energy lifts faster than the LUMO energy upon gate voltage, resulting in the decrease of the energy gap between HOMO and LUMO. Consequently, the energy gap between E_{HOMO} and the Fermi level of electrodes, which governs the electron transport in the BDT molecular junction, is also reduced due to the rise of E_{HOMO} referring to E_F.

Additionally, we calculated the Raman intensities based on the polarizability derivatives in the present of an external electrostatic field. The frequency-dependent polarizability was

DOI: 10.1021/acsnano.8b05826
ACS Nano 2018, 12, 11229−11235

simulated using the adiabatic local density approximation (ALDA) implemented in ADF; see the Supporting Information for detailed information. As shown in Figure 4d, the Raman intensities are gradually enhanced by the gate voltages applied. This result is ascribed to the increasing polarizability derivatives, which is caused by the decrease in the energy gap between the HOMO and the LUMO.[43,44] The selected normal modes of 1,4-benzenedithiol that are responsible for the enhanced Raman signals can be found in Figure S9. The chemical enhancement mechanism predominately contributes to the side-gating enhanced Raman scattering spectra based on the theoretical calculations. The previous work showed that the chemical enhancement is largely governed by the excitation energy and in detail the enhancement factor is inversely proportional to the fourth power of the excitation energy.[42] In molecular junctions, the excitation energy is strongly correlated to the energy gap ($E_{HOMO}-E_{LUMO}$). One can expect that the reduced excitation energy arising from the decreasing energy gap energy leads to the pronounced enhancement of the Raman intensity.

CONCLUSIONS

In summary, we proposed and demonstrated a field-effect Raman scattering (FERS) in a single-molecule junction. To achieve FERS, a nanoscale fabricated gate electrode was integrated to a pair of source-drain electrodes to exert a gating effect on the single-molecule junctions. Combining gating-dependent Raman scattering measurements, tunneling current measurements, and DFT-based calculations, we revealed that Raman scattering can be further enhanced via molecular orbital gating by ~40% beyond the limitation of the electromagnetic enhancement. This finding not only provides a method to increase the sensitivity of Raman scattering but also helps illuminate the enhancement mechanism by two step enhancement process. Additionally, our results demonstrate that gating Raman scattering on single molecules at a target position is feasible. The design of the gate electrode array will allow the realization of an addressable enhancement of Raman scattering which will promote the applications of Raman spectroscopy.

METHODS

Side-Gated Raman Spectroscopy Measurements. The MCBJ sample was fabricated by preparing a suspended gold nanowire with a constriction on a flexible substrate using electron beam lithography and reactive ion etching techniques. This flexible substrate with the suspended metal wire was fixed on a three-point bending apparatus. The push rod (piezo actuated) exerted a bending force on the substrate, and the bending force broke the metal bridge at the smallest constriction, creating two separate nanoelectrodes; see Figure S1. The Raman spectroscopic measurements were performed using a Jobin Yvon system, and the spectra were collected with a confocal Raman microscope equipped with a 100× objective. To reduce the background of the Raman signal, we used Si_3N_4 films instead of the organic insulating films as an insulating film which was normally used for nanofabricated MCBJ samples. Self-assembly of the molecules on the chip surface was performed in a freshly prepared 1 mM solution for 1 h. After self-assembling the molecules on the gold surface, the sample was rinsed with ethanol and dried under a nitrogen stream. The bias voltage was kept at 100 mV during the Raman scattering measurement upon varied gate voltage. The acquisition time was 10 cycles/30 s for each sample.

Electric Field Simulations. The distribution of the electric field as well as the potential were simulated based on the finite-element method (FEM) employing the commercial COMSOL Multiphysics software. To focus on the junction area, the total simulation region was set to 15 nm × 15 nm × 40 nm. To adapt the model as close as possible to the real electrode, the model was built by combining a circular truncated cone with an ellipsoid. The source and drain electrodes were separated by 1.2 nm (approximated to the length of molecule). The perpendicular distance between the gate and the source-drain axis was set to be 8 nm (close to the real fabricated MCBJ chip). A plane wave (wavelength 632.8 nm) from the top of electrode plane impinges on the gold electrodes with a polarization parallel to the electrode−electrode axis. We also performed the simulation using atomistic electrodynamics model, and we obtained the coherent results by employing two different methods (see Figure S5).

Calculations of Raman Spectra under an Electrical Field. In the calculations, the molecule is in contact with the source and drain electrodes through S−Au bonding with in-plane configurations to form an Au/1,4-BDT/Au junction. The geometry optimization was performed using the Becke-Perdew (BP86) functional and Slater-type orbitals represented by triple-polarized (TZP) functions with small frozen cores. The relativistic effects were taken into by means of the scalar zero order regular approximation (ZORA). The frequency-dependent polarizability under an external electric field was simulated using the adiabatic local density approximation (ALDA) implemented in an atomic orbital response module of ADF. The polarizability derivatives were obtained from the numerical three-point differentiation with respect to the normal mode displacement. The calculation of the Raman cross section can be found in the Supporting Information.

ASSOCIATED CONTENT

Supporting Information

The Supporting Information is available free of charge on the ACS Publications website at DOI: 10.1021/acsnano.8b05826.

Detailed information concerning the working principle of the MCBJ device, laser polarization effect to Raman scattering spectroscopy, field distribution upon gating voltage, calculation of Raman cross section (PDF)

AUTHOR INFORMATION

Corresponding Authors

*E-mail: xiangdongde@126.com.
*E-mail: tlee@snu.ac.kr.
*E-mail: bxu@engr.uga.edu.

ORCID

Dirk Mayer: 0000-0003-1296-8265
Takhee Lee: 0000-0001-5988-5219
Dong Xiang: 0000-0002-5632-6355

Author Contributions

[▽]C.G., X.C., and S.-Y.D. have equal contributions to this work.

Notes

The authors declare no competing financial interest.

ACKNOWLEDGMENTS

We are grateful for the financial support from National Natural Science Foundation of China (21303171, 61571242, 11804170). T.L acknowledges National Creative Research Laboratory program (Grant no. 2012026372) through the National Research Foundation of Korea. X.C. acknowledges Advanced CyberInfrastructure computational resources provided by The Institute for CyberScience at The Pennsylvania State University.

DOI: 10.1021/acsnano.8b05826
ACS Nano 2018, 12, 11229−11235

REFERENCES

(1) Cui, L.; Miao, R.; Wang, K.; Thompson, D.; Zotti, L. A.; Cuevas, J. C.; Meyhofer, E.; Reddy, P. Peltier Cooling in Molecular Junctions. *Nat. Nanotechnol.* **2018**, *13*, 122−127.

(2) Kim, Y.; Jeong, W.; Kim, K.; Lee, W.; Reddy, P. Electrostatic Control of Thermoelectricity in Molecular Junctions. *Nat. Nanotechnol.* **2014**, *9*, 881−885.

(3) Schirm, C.; Matt, M.; Pauly, F.; Cuevas, J. C.; Nielaba, P.; Scheer, E. A Current-Driven Single-Atom Memory. *Nat. Nanotechnol.* **2013**, *8*, 645−648.

(4) Xiang, D.; Wang, X.; Jia, C.; Lee, T.; Guo, X. Molecular-Scale Electronics: From Concept to Function. *Chem. Rev.* **2016**, *116*, 4318−4440.

(5) Mitchell, A. K.; Pedersen, K. G. L.; Hedegard, P.; Paaske, J. Kondo Blockade Due to Quantum Interference in Single-Molecule Junctions. *Nat. Commun.* **2017**, *8*, 15210.

(6) Song, H.; Kim, Y.; Jang, Y. H.; Jeong, H.; Reed, M. A.; Lee, T. Observation of Molecular Orbital Gating. *Nature* **2009**, *462*, 1039−1043.

(7) Perrin, M. L.; Verzijl, C. J. O.; Martin, C. A.; Shaikh, A. J.; Eelkema, R.; van Esch, J. H.; van Ruitenbeek, J. M.; Thijssen, J. M.; van der Zant, H. S. J.; Dulic, D. Large Tunable Image-Charge Effects in Single-Molecule Junctions. *Nat. Nanotechnol.* **2013**, *8*, 282−287.

(8) Cui, A.; Dong, H.; Hu, W. Molecular Electronics: Nanogap Electrodes towards Solid State Single-Molecule Transistors. *Small* **2015**, *11*, 6240.

(9) Matsuhita, R.; Horikawa, M.; Naitoh, Y.; Nakamura, H.; Kiguchi, M. Conductance and SERS Measurement of Benzenedithiol Molecules Bridging Between Au Electrodes. *J. Phys. Chem. C* **2013**, *117*, 1791−1795.

(10) Natelson, D.; Li, Y.; Herzog, J. B. Nanogap Structures: Combining Enhanced Raman Spectroscopy and Electronic Transport. *Phys. Chem. Chem. Phys.* **2013**, *15*, 5262−5275.

(11) Benner, D.; Boneberg, J.; Nuernberger, P.; Waitz, R.; Leiderer, P.; Scheer, E. Lateral and Temporal Dependence of the Transport through an Atomic Gold Contact under Light Irradiation: Signature of Propagating Surface Plasmon Polaritons. *Nano Lett.* **2014**, *14*, 5218−5223.

(12) Wang, L.; Wang, L.; Zhang, L.; Xiang, D. Advance of Mechanically Controllable Break Junction for Molecular Electronics. *Top. Curr. Chem.* **2017**, *375*, 61.

(13) Shin, H.-H.; Yeon, G. J.; Choi, H.-K.; Park, S. M.; Lee, K. S.; Kim, Z. H. Frequency-Domain Proof of the Existence of Atomic-Scale SERS Hot-Spots. *Nano Lett.* **2018**, *18*, 262−271.

(14) Iwane, M.; Fujii, S.; Kiguchi, M. Surface-Enhanced Raman Scattering in Molecular Junctions. *Sensors* **2017**, *17*, 1901.

(15) Liu, Z.; Ding, S.-Y.; Chen, Z.-B.; Wang, X.; Tian, J.-H.; Anema, J. R.; Zhou, X.-S.; Wu, D.-Y.; Mao, B.-W.; Xu, X.; Ren, B.; Tian, Z.-Q. Revealing the Molecular Structure of Single-Molecule Junctions in Different Conductance States by Fishing-Mode Tip-Enhanced Raman Spectroscopy. *Nat. Commun.* **2011**, *2*, 305.

(16) Chirumamilla, M.; Toma, A.; Gopalakrishnan, A.; Das, G.; Zaccaria, R. P.; Krahne, R.; Rondanina, E.; Leoncini, M.; Liberale, C.; De Angelis, F.; Di Fabrizio, E. 3D Nanostar Dimers with a Sub-10-nm Gap for Single-/Few- Molecule Surface-Enhanced Raman Scattering. *Adv. Mater.* **2014**, *26*, 2353−2358.

(17) Zhang, R.; Zhang, Y.; Dong, Z. C.; Jiang, S.; Zhang, C.; Chen, L. G.; Zhang, L.; Liao, Y.; Aizpurua, J.; Luo, Y.; Yang, J. L.; Hou, J. G. Chemical Mapping of a Single Molecule by Plasmon-Enhanced Raman Scattering. *Nature* **2013**, *498*, 82−86.

(18) Konishi, T.; Kiguchi, M.; Takase, M.; Nagasawa, F.; Nabika, H.; Ikeda, K.; Uosaki, K.; Ueno, K.; Misawa, H.; Murakoshi, K. Single Molecule Dynamics at a Mechanically Controllable Break Junction in Solution at Room Temperature. *J. Am. Chem. Soc.* **2013**, *135*, 1009−1014.

(19) Marshall, A. R. L.; Stokes, J.; Viscomi, F. N.; Proctor, J. E.; Gierschner, J.; Bouillard, J.-S. G.; Adawi, A. M. Determining Molecular Orientation *via* Single Molecule SERS in a Plasmonic Nano-Gap. *Nanoscale* **2017**, *9*, 17415−17421.

(20) Witlicki, E. H.; Johnsen, C.; Hansen, S. W.; Silverstein, D. W.; Bottomley, V. J.; Jeppesen, J. O.; Wong, E. W.; Jensen, L.; Flood, A. H. Molecular Logic Gates Using Surface-Enhanced Raman-Scattered Light. *J. Am. Chem. Soc.* **2011**, *133*, 7288−7291.

(21) Jiang, S.; Zhang, Y.; Zhang, R.; Hu, C. R.; Liao, M. H.; Luo, Y.; Yang, J. L.; Dong, Z. C.; Hou, J. G. Distinguishing Adjacent Molecules on a Surface Using Plasmon-Enhanced Raman Scattering. *Nat. Nanotechnol.* **2015**, *10*, 865−869.

(22) Ciraci, C.; Hill, R. T.; Mock, J. J.; Urzhumov, Y.; Fernandez-Dominguez, A. I.; Maier, S. A.; Pendry, J. B.; Chilkoti, A.; Smith, D. R. Probing the Ultimate Limits of Plasmonic Enhancement. *Science* **2012**, *337*, 1072−1074.

(23) Herzog, J. B.; Knight, M. W.; Li, Y.; Evans, K. M.; Halas, N. J.; Natelson, D. Dark Plasmons in Hot Spot Generation and Polarization in Interelectrode Nanoscale Junctions. *Nano Lett.* **2013**, *13*, 1359−1364.

(24) Xu, H.; Xie, L.; Zhang, H.; Zhang, J. Effect of Graphene Fermi Level on the Raman Scattering Intensity of Molecules on Graphene. *ACS Nano* **2011**, *5*, 5338−5344.

(25) van Schrojenstein Lantman, E. M.; Deckert-Gaudig, T.; Mank, A. J. G.; Deckert, V.; Weckhuysen, B. M. Catalytic Processes Monitored at the Nanoscale with Tip-Enhanced Raman Spectroscopy. *Nat. Nanotechnol.* **2012**, *7*, 583.

(26) Saito, R.; Sato, K.; Araujo, P. T.; Mafra, D. L.; Dresselhaus, M. S. Gate Modulated Raman Spectroscopy of Graphene and Carbon Nanotubes. *Solid State Commun.* **2013**, *175*, 18−34.

(27) Cui, L.; Liu, B.; Vonlanthen, D.; Mayor, M.; Fu, Y. C.; Li, J. F.; Wandlowski, T. *In Situ* Gap-Mode Raman Spectroscopy on Single-Crystal Au(100) Electrodes: Tuning the Torsion Angle of 4,4 '-Biphenyldithiols by an Electrochemical Gate Field. *J. Am. Chem. Soc.* **2011**, *133*, 7332−7335.

(28) Matsushita, R.; Kiguchi, M. Surface Enhanced Raman Scattering of a Single Molecular Junction. *Phys. Chem. Chem. Phys.* **2015**, *17*, 21254−21260.

(29) Wang, Q.; Liu, R.; Xiang, D.; Sun, M.; Zhao, Z.; Sun, L.; Mei, T.; Wu, P.; Liu, H.; Guo, X.; Li, Z.-L.; Lee, T. Single-Atom Switches and Single-Atom Gaps Using Stretched Metal Nanowires. *ACS Nano* **2016**, *10*, 9695−9702.

(30) Xiang, D.; Jeong, H.; Kim, D.; Lee, T.; Cheng, Y. J.; Wang, Q. L.; Mayer, D. Three-Terminal Single-Molecule Junctions Formed by Mechanically Controllable Break Junctions with Side Gating. *Nano Lett.* **2013**, *13*, 2809−2813.

(31) Wagner, S.; Kisslinger, F.; Ballmann, S.; Schramm, F.; Chandrasekar, R.; Bodenstein, T.; Fuhr, O.; Secker, D.; Fink, K.; Ruben, M.; Weber, H. B. Switching of a Coupled Spin Pair in a Single-Molecule Junction. *Nat. Nanotechnol.* **2013**, *8*, 575−579.

(32) Tian, J. H.; Liu, B.; Li, X. L.; Yang, Z. L.; Ren, B.; Wu, S. T.; Tao, N. J.; Tian, Z. Q. Study of Molecular Junctions with a Combined Surface-Enhanced Raman and Mechanically Controllable Break Junction Method. *J. Am. Chem. Soc.* **2006**, *128*, 14748−14749.

(33) Zrimsek, A. B.; Chiang, N. H.; Mattei, M.; Zaleski, S.; McAnally, M. O.; Chapman, C. T.; Henry, A. I.; Schatz, G. C.; Van Duyne, R. P. Single-Molecule Chemistry with Surface- and Tip-Enhanced Raman Spectroscopy. *Chem. Rev.* **2017**, *117*, 7583−7613.

(34) Tsutsui, M.; Taniguchi, M.; Kawai, T. Single-Molecule Identification *via* Electric Current Noise. *Nat. Commun.* **2010**, *1*, 138.

(35) Wu, S. M.; Gonzalez, M. T.; Huber, R.; Grunder, S.; Mayor, M.; Schonenberger, C.; Calame, M. Molecular Junctions Based on Aromatic Coupling. *Nat. Nanotechnol.* **2008**, *3*, 569−574.

(36) Liu, C.; Kaneko, S.; Komoto, Y.; Fujii, S.; Kiguchi, M. Highly Conductive Single Naphthalene and Anthracene Molecular Junction with Well-Defined Conductance. *Appl. Phys. Lett.* **2015**, *106*, 103103.

(37) Zhao, Z.; Liu, R.; Mayer, D.; Coppola, M.; Sun, L.; Kim, Y.; Wang, C.; Ni, L.; Chen, X.; Wang, M.; Li, Z.; Lee, T.; Xiang, D. Shaping the Atomic-Scale Geometries of Electrodes to Control Optical and Electrical Performance of Molecular Devices. *Small* **2018**, *14*, 1703815.

DOI: 10.1021/acsnano.8b05826
ACS Nano 2018, 12, 11229−11235

(38) Zhu, W.; Crozier, K. B. Quantum Mechanical Limit to Plasmonic Enhancement as Observed by Surface-Enhanced Raman Scattering. *Nat. Commun.* **2014**, *5*, 5228.
(39) Savage, K. J.; Hawkeye, M. M.; Esteban, R.; Borisov, A. G.; Aizpurua, J.; Baumberg, J. J. Revealing the Quantum Regime in Tunnelling Plasmonics. *Nature* **2012**, *491*, 574−577.
(40) Hajisalem, G.; Nezami, M. S.; Gordon, R. Probing the Quantum Tunneling Limit of Plasmonic Enhancement by Third Harmonic Generation. *Nano Lett.* **2014**, *14*, 6651−6654.
(41) Xiang, D.; Jeong, H.; Lee, T.; Mayer, D. Mechanically Controllable Break Junctions for Molecular Electronics. *Adv. Mater.* **2013**, *25*, 4845−4867.
(42) Morton, S. M.; Jensen, L. Understanding the Molecule-Surface Chemical Coupling in SERS. *J. Am. Chem. Soc.* **2009**, *131*, 4090−4098.
(43) Verma, P. Tip-Enhanced Raman Spectroscopy: Technique and Recent Advances. *Chem. Rev.* **2017**, *117*, 6447−6466.
(44) Ding, S.; Ren, B.; Tian, Z. An Ion-Modified Cluster Model for Studying the Correlation of Raman Intensity and Electric Conductance of Single Molecule in the Molecular Junction. *Zhongguo Kexue: Huaxue* **2018**, *48*, 196−203.

DOI: 10.1021/acsnano.8b05826
ACS Nano 2018, 12, 11229−11235